

Received September 30, 2019, accepted October 13, 2019, date of publication October 18, 2019, date of current version October 30, 2019.

Digital Object Identifier 10.1109/ACCESS.2019.2948213

Simultaneous Distributed Vibration and Temperature Sensing Using Multicore Fiber

YUNLI DANG¹, ZHIYONG ZHAO^{1b2}, XUEFENG WANG³, RUOLIN LIAO^{1b3}, AND CHAO LU²

¹State Key Laboratory of Optical Fiber and Cable Manufacture Technology, Research and Development Department, Yangtze Optical Fiber and Cable Joint Stock Limited Company (YOF), Wuhan 430073, China

²Department of Electronic and Information Engineering, The Hong Kong Polytechnic University, Hong Kong

³School of Optical and Electronic Information, Huazhong University of Science and Technology, Wuhan 430074, China

Corresponding author: Zhiyong Zhao (zhiyong.zhao@polyu.edu.hk)

This work was supported in part by the National Key Research and Development Program of China under Grant 2017YFB0405500, in part by the National Natural Science Foundation of China under Grant 61435006 and Grant U1701661, and in part by the GRF under Grant PolyU 152168/17E and Grant PolyU 152658/16E of research grant council, Hong Kong SAR, and 1-ZVGB, 1-YW3G, and 4-BCCK of the Hong Kong Polytechnic University.

ABSTRACT Distributed optical fiber sensing that enables simultaneous vibration and temperature monitoring is demonstrated in this work, which is achieved by implementing polarization optical time-domain reflectometry (P-OTDR) and Raman optical time-domain reflectometry (ROTDR) respectively through space-division multiplexed (SDM) configuration in different cores of a multicore fiber (MCF). Optimized system setup is obtained in the proposed hybrid system, where only one laser source is used, and the generated pulse is shared by the two reflectometers. Owing to the reason that separate interrogation fiber cores are used by the two reflectometers, the proposed hybrid system allows for simultaneous measurements of spontaneous Raman and Rayleigh scattering signals, thus it no longer suffers from the incompatible pump power levels issue, which results from different pump power demands, and hinders the implementation of the hybrid system in single mode fiber due to the fiber nonlinear effects imposed restriction. In addition, in order to extend the sensing range, we also explore the employment of wavelet transform denoising technique in the improvement of signal-to-noise ratio of ROTDR measurement. Eventually, simultaneous distributed vibration and temperature sensing in 5.76 km sensing range with 3 m spatial resolution and 0.57 °C temperature uncertainty has been demonstrated. The proposed hybrid sensing system has the outstanding advantage of high reliability, since the cross-sensitivity issue is effectively mitigated, which shows great potential for pipeline monitoring in oil and gas industry.

INDEX TERMS Multicore fiber, space-division multiplexing, distributed temperature sensing, distributed vibration sensing.

I. INTRODUCTION

The intelligent monitoring of environmental variation in the fields of civil, mining, and energy exploration has attracted ever increasing attention recently, where the environmental parameters (e.g. vibration, temperature and strain, etc.) are utilized to perceive the structure integrity and health condition, so that the safety and reliability of industrial operations can be enhanced notably. Specifically, simultaneous vibration and temperature sensing are highly desired for long range and distributed pipeline monitoring in oil and gas industry [1], [2], which can be used for intrusion detection and leakage detection, respectively. Distributed optical fiber sensing (DOFS)

The associate editor coordinating the review of this manuscript and approving it for publication was Pinjia Zhang.

technique based on the measurements of backscattering signals turns out to be one of the most promising solutions for this application, thanks to its outstanding capability of long sensing range (tens of kilometers) and high spatial resolution (meter-scale) [3]. However, it is difficult to achieve simultaneous and discriminative measurement between vibration and temperature by using a single distributed fiber sensing technique, because most of the DOFS techniques are suffering from the cross-sensitivity issue among multiple parameters, which will decrease dramatically the reliability of measurements in real field deployment. One solution of this problem is to use two sensing techniques simultaneously, where one is used to monitor vibration, meanwhile the other one can be utilized to sense temperature.

Although Brillouin distributed fiber sensors have been widely used for temperature and strain measurement [4], the technique is however inherent sensitive to both parameters, which leads to difficulty in the determination of disturbances in practical applications [5]. On the contrary, Raman optical time-domain reflectometry (ROTDR) is only sensitive to temperature, but not strain or vibration, so it is a very good option for temperature sensing in the hybrid system. On the other hand, although phase-sensitive optical time-domain reflectometry (φ -OTDR) has been widely employed for vibration sensing [6]–[8], the technology is however also ultrasensitive to temperature change with a temperature sensitivity of approximately 1.3 GHz/°C @ 1550 nm in the normal silica fiber as has been quantified from the local coherent Rayleigh interference spectrum through cross-correlation [9]–[12]. So it turns out that the sensor will subject to serious impact of environmental temperature change in realistic deployment scenario, since vibration detection based on φ -OTDR relies on the monitoring of local Rayleigh backscattering optical intensity/phase variation, so even if slow environmental temperature change will still lead to remarkable intensity/phase variation due to its ultrahigh temperature sensitivity, as a result it might cause frequent false alarms, so the reliability of measurement is not good. In fact, in addition to φ -OTDR, polarization optical time-domain reflectometry (P-OTDR) has also been intensively used for vibration detection [13]–[17]. The advantage of P-OTDR is that it has pretty low temperature dependence; so it won't be dramatically affected by the environmental temperature change; eventually the reliability of P-OTDR for vibration detection will be better than that uses φ -OTDR. Hence it turns out that P-OTDR is preferred for vibration detection in the proposed hybrid sensing system for the consideration of reliability. In this case, the proposed hybrid sensing system will no longer suffer from the cross-sensitivity issue.

However, it is difficult to implement the hybrid P-OTDR and ROTDR sensing system simultaneously in a single mode fiber (SMF), because the spontaneous Raman scattering signal (SpRS) in optical fiber is very weak, normally very high pump power is required for ROTDR (typically a few Watts) and avalanche photodiode is needed for the detection of SpRS. However, high pump power will cause nonlinear effects in the fiber, including modulation instability, stimulated Brillouin scattering [18]–[23], etc. The onset of nonlinear effects will distort the trace of Rayleigh backscattering by an abruptly dropping of the backscattering optical intensity, which leads to significant reduction of visibility and eventually hinders the measurement of P-OTDR. On the other hand, the tolerance of ROTDR to nonlinear effects is much higher than the Rayleigh backscattering enabled P-OTDR, since both Raman Stokes and anti-Stokes components are spectrally far away from the pump light. Therefore, it turns out that it is difficult to achieve simultaneous measurements of P-OTDR and ROTDR in a single SMF due to the incompatible pump power demands between the two sensors, especially

when the fiber length is very long. In order to carry out P-OTDR and ROTDR simultaneously, a feasible solution is to multiplex the two sensors spatially in different cores of a multicore fiber, in which different pump powers are injected, so that the incompatible pump power levels issue can be addressed.

In this paper, we propose and experimentally demonstrate a multicore fiber (MCF) spatially multiplexed P-OTDR and ROTDR hybrid sensing system, where P-OTDR is used for vibration detection and ROTDR is employed for temperature monitoring. Thanks to the separate implementation of the two sensors, simultaneous measurement of spontaneous Raman and Rayleigh scattering signals is enabled, as a result the proposed hybrid sensing system achieves simultaneous distributed vibration and temperature monitoring with negligible cross-sensitivity. Besides, in order to improve the signal-to-noise ratio (SNR) of the measured Raman backscattering signals, wavelet transform based denoising technique is used, which contributes to significant SNR improvement and consequently considerable temperature uncertainty decline. The proposed hybrid sensing system with high reliability turns out to be a promising solution for pipelines monitoring in oil and gas industry.

II. WORKING PRINCIPLES OF THE PROPOSED HYBRID SENSING SYSTEM

In the proposed spatially multiplexed hybrid sensing system, ROTDR is only sensitive to temperature, but not strain or vibration. ROTDR is able to measure temperature along the whole fiber length, which relies on the temperature dependence of Raman anti-Stokes signal. Temperature profile can be extracted from the power ratio of Raman anti-Stokes ($I_{as}(z)$) to Stokes ($I_s(z)$) light, according to

$$\frac{I_{as}(z)}{I_s(z)} \propto \left(\frac{\lambda_s}{\lambda_{as}} \right)^4 \exp\left(-\frac{h\Delta\nu}{k_B T(z)}\right) \quad (1)$$

where λ_s , λ_{as} are the wavelength of Raman Stokes and anti-Stokes light, respectively; h is the Planck constant; $\Delta\nu$ is the frequency separation between the pump and Raman signals; k_B is the Boltzmann constant, and $T(z)$ is the fiber temperature.

On the other hand, distributed vibration sensing can be achieved by P-OTDR, which relies on monitoring the state of polarization (SOP) of Rayleigh backscattering signal along a fiber. External vibration applied to the sensing fiber modifies the local birefringence of fiber, which results in a variation of SOP. A polarizer is typically used at the receiver side before the detector, so as to convert the modification of SOP to the variation of optical intensity. Therefore, intrusion can be detected by monitoring the change of output power in P-OTDR sensors. Specifically, the fiber can be modeled by cascaded wave plates with linear birefringence [15], where polarization-dependent loss is neglected. The forward Muller matrix of each segment of birefringence wave plate is given

by [15], [24], [25]

$$M_i = \alpha \begin{bmatrix} 1 & 0 & 0 & 0 \\ 0 & m_{11} & m_{12} & m_{13} \\ 0 & m_{21} & m_{22} & m_{23} \\ 0 & m_{31} & m_{32} & m_{33} \end{bmatrix} \quad (2)$$

And the elements of Eq. (2) are given by

$$\begin{aligned} m_{11} &= \cos^2 2\theta_i + \sin^2 2\theta_i \cos \delta_i \\ m_{12} &= m_{21} = \cos 2\theta_i \sin 2\theta_i (1 - \cos \delta_i) \\ m_{13} &= -m_{31} = -\sin 2\theta_i \sin \delta_i \\ m_{22} &= \sin^2 2\theta_i + \cos^2 2\theta_i \cos \delta_i \\ m_{23} &= -m_{32} = \cos 2\theta_i \sin \delta_i \\ m_{33} &= \cos \delta_i \end{aligned} \quad (3)$$

where θ_i is the angle between the fast axis and the local x -axis and δ_i is the phase delay between the x -axis and the y -axis in the i -th wave plate; α is the attenuation coefficient of the wave plate. Then the Muller matrix of backward Rayleigh scattering light of n cascaded wave plates is governed by

$$M_B(n) = R(M_n, \dots, M_2 M_1)^T R(M_n, \dots, M_2 M_1) \quad (4)$$

where $R = \text{diag}(1, 1, 1, -1)$. Since the coherent length of the used laser source in POTDR is normally much shorter than the fiber length l that the pulse duration takes up, the backscattered light within the pulse width will superimpose at the receiver, and the Stokes vector of the received light is governed by

$$S_{out}(z) = r \sum_{n=z-l/2}^z M_B(n) \cdot S_{in} \quad (5)$$

where r is the coefficient of Rayleigh backscattering, z is the location of pulse front edge, and S_{in} is the Stokes vector of input light. Assuming that the polarization axis of the polarizer is parallel to the local x -axis, then the detected optical intensity after the polarizer is determined by

$$I = \frac{S_{out0} + S_{out1}}{2} \quad (6)$$

where S_{out0} and S_{out1} are two Stokes parameters of the Stokes vector S_{out} . When perturbation is applied to the sensing fiber, the local birefringence of fiber will be modified, so that Muller matrix will change accordingly, as a result the output power after the polarizer will vary as well, and thus the perturbation event can be detected.

Different from φ -OTDR where narrow linewidth coherent laser is required, P-OTDR should not use very narrow-linewidth laser source in order to avoid the occurrence of coherent Rayleigh interference. On the other hand, the linewidth of the laser cannot be too wide, in order to prevent the frequency domain depolarization effect, which stems from different polarization transformations of various frequency components in the light source [15]. As a result, the laser source used in P-OTDR typically has a linewidth in the range of tens of GHz. Such a specific laser source

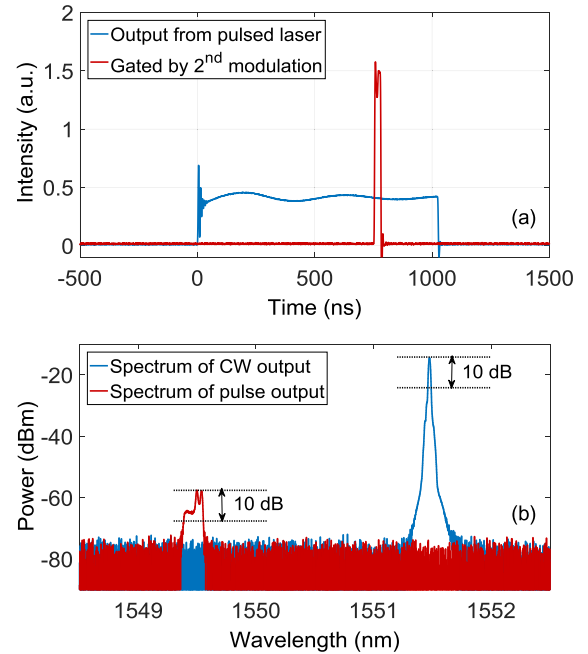


FIGURE 1. (a) The measured temporal pulse waveforms; (b) the measured spectra of the laser with CW output and pulsed output, respectively.

can be obtained by directly modulating a distributed-feedback (DFB) laser with dithering current.

Thanks to the proposed novel space-division multiplexed system setup, the incompatible pump power demands issue of the hybrid system can be addressed effectively. This will allow for simultaneous interrogation of spontaneous Raman and Rayleigh scattering signals, which makes simultaneous vibration and temperature monitoring in only one sensing fiber possible.

III. EXPERIMENTAL SETUP, RESULTS AND DISCUSSIONS

A. DIRECTLY MODULATED DFB LASER WITH DITHERING CURRENT

In order to get a laser source that applies to P-OTDR, a home-made drive circuit has been developed to directly modulate the DFB laser, where dithering current is employed with 1020 ns pulse duration. The output from the pulsed laser after direct modulation is then externally modulated again with 30 ns pulse width to get a narrow pulse, which enables high spatial resolution for the measurement of P-OTDR and ROTDR. The temporal pulse waveforms measured from the output of the directly modulated laser and external modulator have been presented in Fig. 1(a). It is well known that dithering current will broaden the linewidth of the laser. To verify this, the output spectra of laser operating in CW mode and pulse mode after direct modulation have been experimentally compared, as shown in Fig. 1(b). The 10-dB linewidths are measured to be 0.03 nm and 0.17 nm, respectively. It should be pointed out that the resolution of the used optical spectrum analyzer (OSA) is 0.02 nm. The reason why wavelength shifts is that different driving currents are employed for the two

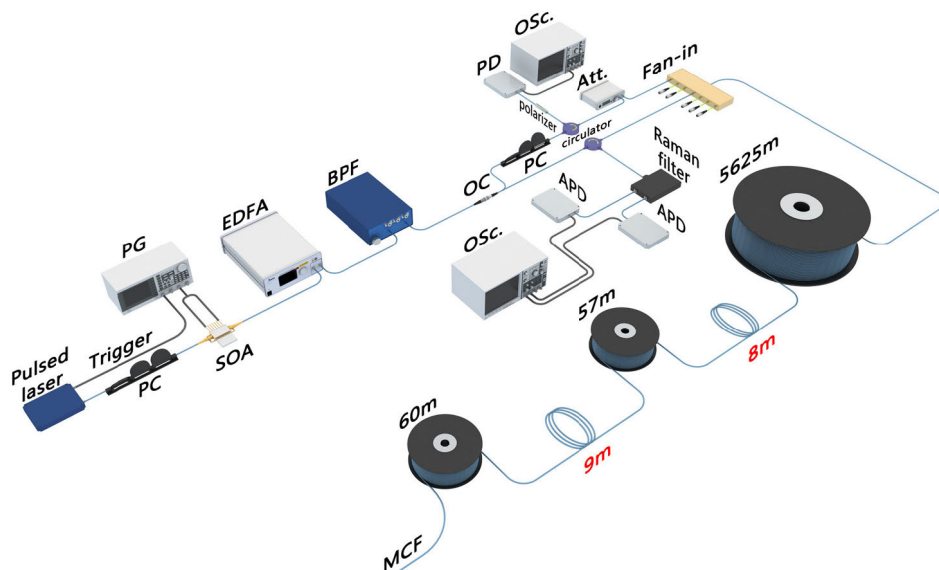


FIGURE 2. Experimental setup of the proposed spatially multiplexed P-OTDR and ROTDR hybrid sensing system. PC: polarization controller; PG: pulse generator; SOA: semiconductor optical amplifier; EDFA: erbium-doped fiber amplifier; BPF: band-pass filter; OC: optical coupler; Att.: tunable attenuator; PD: photodiode; APD: avalanche photodiode; Osc.: oscilloscope.

operating modes. In this way, the well-tailored laser source will be suitable for P-OTDR in the SDM hybrid sensing system now.

B. EXPERIMENTAL SETUP

The experimental setup of the proposed spatially multiplexed P-OTDR and ROTDR hybrid sensor based on MCF is shown in Fig. 2. The pulsed laser generates a 1020 ns optical pulse, and then a semiconductor optical amplifier (SOA) is used for the external modulation of the output from the directly modulated laser, and the SOA is driven by a pulse generator with 30 ns electrical pulse width. The gated pulse is then amplified by an erbium-doped fiber amplifier (EDFA), which is followed by a bandpass filter so as to filter out the ASE noise. Then light is divided into two branches through a 50:50 optical coupler. The pulse in the upper branch goes through a circulator and a tunable attenuator, and eventually it is launched into one of the outer cores through the fan-in coupler. The attenuator is used to control the peak power of the pulse in order to suppress the onset of nonlinear effects (e.g. modulation instability) in the fiber link. At the receiver side, a polarizer is employed before the photodiode. The other branch is used for the implementation of ROTDR with the pulse being injected into the central core of the MCF. The backscattered Raman Stokes and anti-Stokes components are separated by a Raman filter and finally detected by two 125 MHz avalanche photodiode (APD) detectors. The detectors are connected to an oscilloscope for data acquisition with 100 MS/s sampling rate.

As shown in Fig. 3, the MCF has a cladding diameter of 150 μm, and the core-core pitch is 42 μm. The outer six cores are arranged hexagonally, and all cores are surrounded by deep trench claddings in order to suppress the

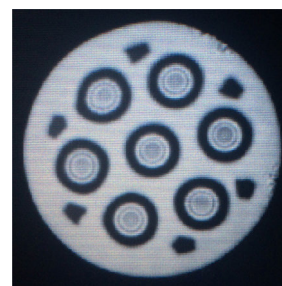


FIGURE 3. Cross section view of the seven-core fiber that is used in the experiment.

crosstalk between adjacent cores. Additionally, the six black holes close to the boundary of the cladding are made of low reflective index material, which was used to fill the tube when stack the preform during the fiber fabrication process, so that all-solid fiber structure can be achieved, and it will ensure good mechanical robustness of the fiber.

It is worth mentioning that a fiber that consists of two cores will be sufficient for the proposed hybrid sensing system, but since we don't have a two-core fiber in the lab, for proof of concept, a MCF containing seven cores has been used in our experiment. It should also be pointed out that it is difficult to obtain comparable performance by using multiple independent single mode fibers. The shortcoming of using separated SMFs is that it is very likely to cause positioning misalignment between different sensing fibers. While it is not a problem for MCF because the cores of MCF have strictly identical physical paths along the fiber length. In addition, MCF has some other advantages, including simpler and more robust sensor design, ease of installation, reduced costs in terms of embedding or attaching the sensors, etc.

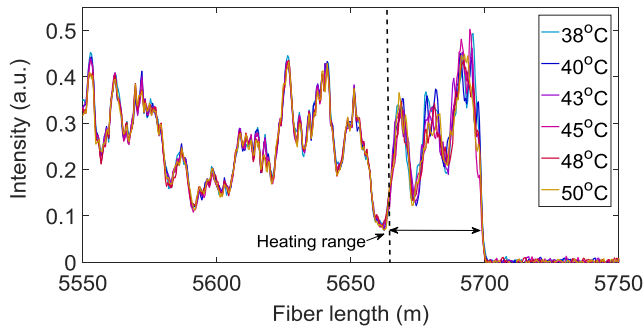


FIGURE 4. Evolution of the measured P-OTDR traces when different temperatures are applied to the last 35-meter sensing fiber at the far end.

C. COMPARISON OF TEMPERATURE SENSITIVITY BETWEEN P-OTDR AND φ -OTDR

Although both φ -OTDR and P-OTDR have been widely used for distributed vibration sensing, the technique used for vibration detection in the proposed system should have low temperature cross-sensitivity, so that high measurement reliability can be ensured. Therefore, firstly it is necessary to compare the performance of φ -OTDR and P-OTDR on temperature dependence by characterizing their temperature sensitivities.

Firstly, the last 35-meter sensing fiber at the far end has been immersed into a water bath, and temperature is varied by electrical heating with an increment of 2 °C or 3 °C. The measured P-OTDR traces under different temperatures are presented in Fig. 4, where 512 times average is used in order to achieve good SNR of measurement. Due to the random distribution of birefringence in optical fiber, the SOP varies randomly as well, as a result the detected optical power after the polarizer exhibits random intensity fluctuation, as can be seen from the figure. In addition, since the traces are acquired when different temperatures are applied at the fiber end, it is also observed from the figure that the traces within the heating range vary with temperature, but the intensity variation is actually small even with a large temperature change. The low sensitivity of P-OTDR on temperature may be due to the reason that the used fiber has all-solid silica fiber core structure, as a result the temperature induced birefringence variation is minor, and so the temperature sensitivity of P-OTDR is low.

For comparison, we also characterized the temperature response of a conventional φ -OTDR, in which a narrow linewidth (1 kHz) coherent laser was employed, and we used the same type of MCF but with a length of 2.95 km. The last 37 m long fiber was heated by immersing into a water bath. The measured φ -OTDR traces around the fiber end are shown in Fig. 5, where seven traces are plotted. The seven traces were collected during the heating process, and they were sampled every eight seconds, the total temperature change during this period is about 1 °C. It is observed from Fig. 5 that the seven traces are almost completely coincident except for the heating range, and it is quite obvious that temperature change will cause severe intensity fluctuation at the heating range of

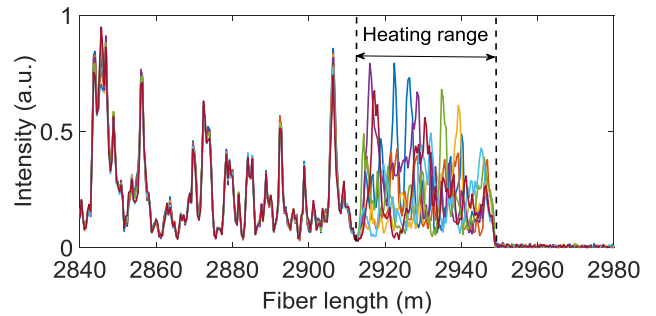


FIGURE 5. Overlapped φ -OTDR traces of seven measurements that were acquired when the last 37 m long fiber was heated. The traces are sampled every eight seconds, and the total temperature increment during this period is about 1 °C.

φ -OTDR traces, even though just with a small temperature variation, i.e. 1 °C in this case.

So it indicates that although P-OTDR trace is temperature dependent, it is apparently much less sensitive than φ -OTDR. The ultrahigh temperature sensitivity of φ -OTDR will reduce significantly its reliability of vibration detection. While on the other hand, since temperature change caused intensity fluctuation is small in P-OTDR sensor, as indicated by Fig. 4, so the impact can be effectively eliminated by setting an appropriate threshold value of differential intensity variation that is used for event identification and alarm. Therefore, it turns out that temperature change won't degrade dramatically the sensing reliability of P-OTDR.

D. VIBRATION DETECTION USING P-OTDR IN THE PROPOSED HYBRID SENSING SYSTEM

On the other hand, vibration will cause deformation of the sensing fiber due to vibration induced fiber curvature change or transverse loading force, which will change the local birefringence of fiber and consequently results in a variation of SOP, so the output power will change, as shown in Fig. 6, which presents the detected traces measured by P-OTDR without and with intrusion applied to the fiber segment near the end of MCF.

It is worth mentioning that the P-OTDR is implemented in an off-center core in the hybrid system. The benefit of using an off-center core is that it is sensitive to bending [26]. Since vibration induced displacement will cause fiber bending, which will change the birefringence of off-center cores. But in contrast the core of a normal single mode fiber is located in the geometric neutral axis of the fiber; it is not sensitive to bending at all. Therefore, off-center cores will contribute to providing enhanced sensitivity of vibration detection in comparison with the one using the normal single mode fiber whose core is in the geometric center.

Based on such a feature, intrusion event can be detected from the differential optical intensity profile, which can be obtained by subtracting the measured traces with a reference trace. In the experiment, intrusion is emulated by manually tapping on the sensing fiber near the far end. Simultaneously, the P-OTDR traces are consecutively recorded. The mapping

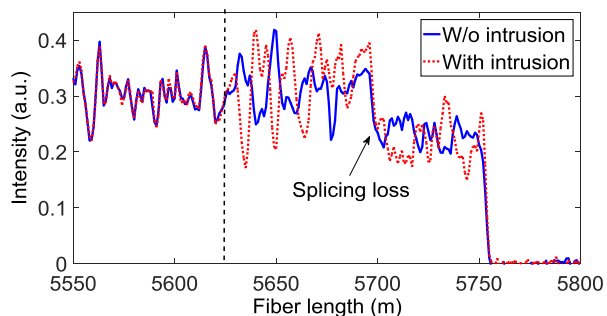


FIGURE 6. The measured P-OTDR traces without and with intrusion applied to the fiber segment near the end of MCF, respectively.

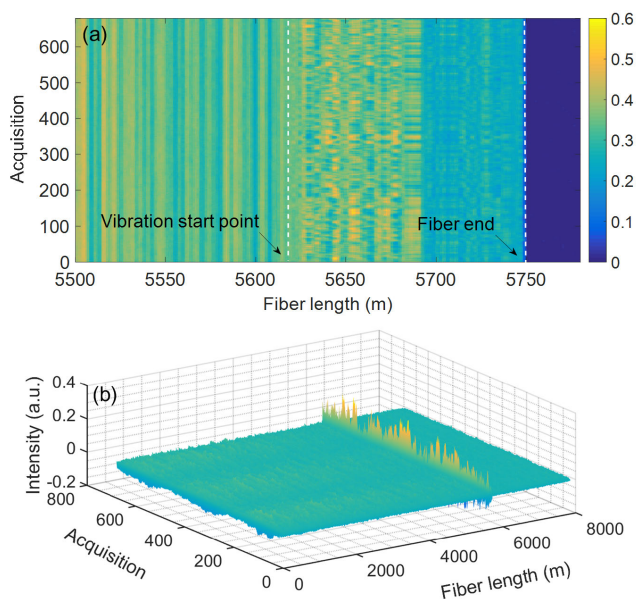


FIGURE 7. (a) Mapping of the acquired P-OTDR traces as a function of acquisition times and distance; (b) evolution of the differential optical intensity as a function of acquisition times and distance.

of the acquired P-OTDR traces as a function of acquisition times and distance is shown in Fig. 7(a), where the vibration start location has been marked. As can be seen, the measured optical power will remain constant at the undisturbed region, while the optical intensity will change as time if perturbation is applied. Fig. 7(b) shows the evolution of differential intensity that is obtained by subtracting the raw traces with a reference trace (e.g. the first acquired trace), where significant intensity variation can be observed at the disturbed region. By this means, intrusion event can be monitored from the differential intensity profile once an appropriate threshold value is set.

The pulse repetition ratio is 10 kHz in our experiment. Therefore, theoretically the maximum detectable vibration frequency is 5 kHz according to the sampling theorem. In order to evaluate the performance of vibration frequency sensing, experiments have also been implemented to investigate the response of P-OTDR on periodic vibration. A short section of fiber at the far end is wound to a piezoelectric transducer (PZT), and the PZT is driven by an arbitrary waveform generator. Then vibration with different frequencies

has been applied to the sensing fiber, meanwhile the time-domain traces of P-OTDR are recorded. The measured time-domain waveforms as a function of time and fiber length when vibrations with frequency of 100 Hz, 1 kHz and 5 kHz are applied to the sensing fiber are presented in Fig. 8(a), 8(b) and 8(c), respectively. Fig. 8(d), 8(e) and 8(f) show the calculated frequency spectrums by processing the sampled data of Fig. 8(a), 8(b) and 8(c) with fast Fourier transform (FFT), respectively. The result verifies that the measured vibration frequencies match well with the applied values, and it also confirms that the maximum detectable vibration frequency of P-OTDR in the hybrid system is 5 kHz.

Here, it is worth mentioning that in order to achieve multi-point vibration detection using P-OTDR in the hybrid system, several methods can be employed, e.g. using the fast Fourier transform spectrum analysis method [13], employing two-dimensional image processing and statistical clustering method [16], and using probe pulses with ergodic states of polarization [27], etc.

E. TEMPERATURE MONITORING USING ROTDR IN THE PROPOSED HYBRID SENSING SYSTEM

On the other hand, the measurement of ROTDR is carried out in parallel in the central core, which is dedicated to achieving distributed temperature sensing, thus simultaneous distributed vibration and temperature detection is enabled by using the proposed hybrid system. Here, the performance of ROTDR using the linewidth broadened laser has also been evaluated.

Due to the fact that the spontaneous Raman scattering signal is very weak in optical fibers, as a result the sensing length of ROTDR is normally short, typically around 10 km. In order to extend the sensing range, a good way is to process the acquired raw data by adopting denoising technique in order to enhance the SNR of measurement [28]. Since the MCF used in this experiment is only 5.76 km, low pump power has been intentionally used for ROTDR in the experiment so as to generate bad SNR to emulate the scenario of a long range ROTDR system, and then wavelet transform based denoising technique is applied to improve the SNR of signal. Wavelet transform is a widely used signal process technique for image denoising, which decomposes a raw signal into weighted sets of scales that represent different frequency bands, then soft thresholding is applied to remove the unwanted noise frequency components, and eventually reconstruction of the signal can be obtained through inverse wavelet transform [29], [30].

The pump power used for R-OTDR in this setup is 30.6 dBm. The measured raw Raman anti-Stokes trace together with the denoised trace are shown in Fig. 9, whose vertical axis is showing in logarithmic scale, and the inset shows the complete Raman anti-Stokes trace with linear scale of the vertical axis. It is observed that the noise induced intensity fluctuation of the signal has been significantly suppressed after denoising, which will contribute to significant SNR improvement. For verification, the SNRs of the raw trace and

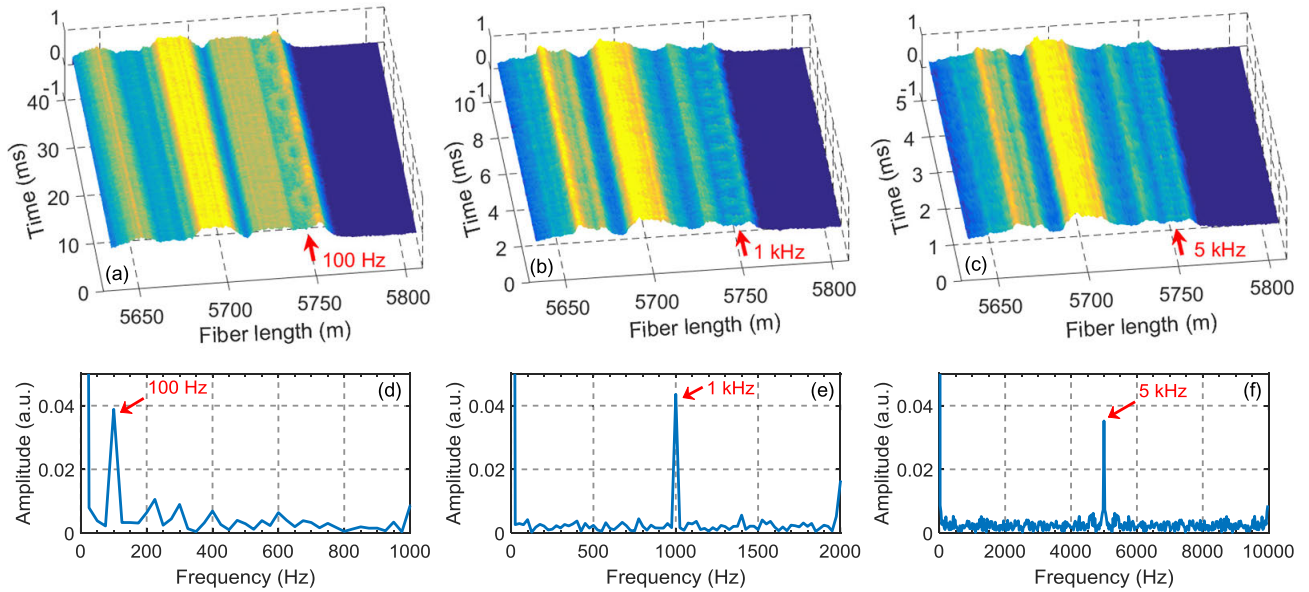


FIGURE 8. The measured time-domain waveforms as a function of time and fiber length when vibration with frequency of (a) 100 Hz, (b) 1 kHz and (c) 5 kHz is applied to the sensing fiber at the far end. (d), (e) and (f) are the retrieved frequency spectrums calculated from (a), (b) and (c), respectively.

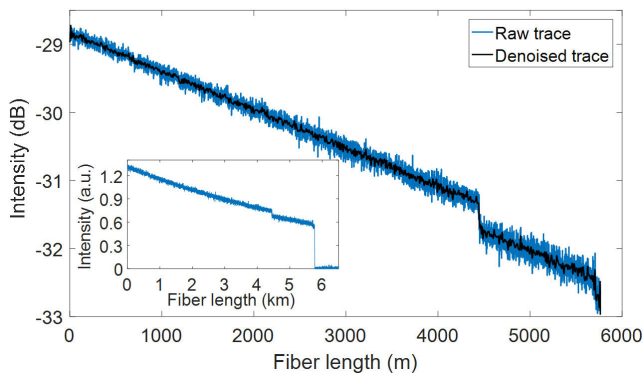


FIGURE 9. The measured raw Raman anti-Stokes trace in blue purple and the denoised trace in black. The inset shows the measured complete Raman anti-Stokes trace with linear vertical axis.

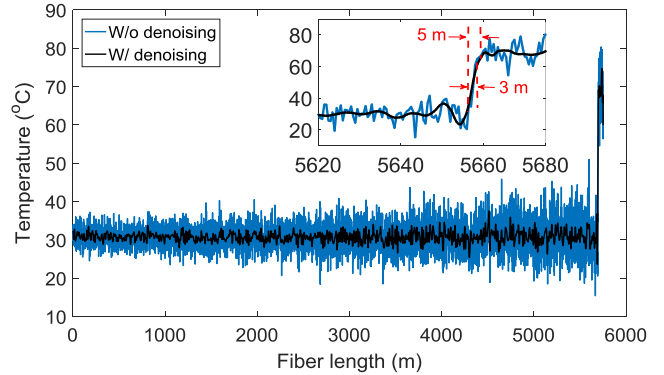


FIGURE 10. The resolved temperature distributions along the sensing fiber by using the raw data (blue purple line) and the denoised data (black line); the inset shows the zoom-in view around the hot-spot at the fiber end.

the denoised trace are then calculated, and it indicates that 5.1 dB SNR enhancement is achieved at the end of the sensing fiber after denoising. The huge SNR improvement will help to reduce notably the temperature uncertainty.

In order to verify the performance enhancement of ROTDR in the proposed hybrid system, the temperature distribution profiles along the sensing fiber that are retrieved from both the raw data and the denoised data have been presented in Fig. 10. Note that a hot-spot is generated at the far end of the sensing fiber, where the last 60 m long fiber is heated to 70 °C. It is observed from Fig. 10 that the resolved temperature profile from the denoised data becomes much smoother in comparison with that from the raw data. The much reduced profile fluctuation will help notably to decrease the uncertainty of temperature measurement.

While it should be mentioned that due to the processing of wavelet transform denoising, the spatial resolution of system is degraded from 3 m to 5 m, as shown in the inset of Fig. 10.

In order to effectively mitigate the degradation of spatial resolution that results from denoising processing, higher sampling rate and less amount of SNR improvement should be adopted [31].

To validate the effectiveness of the denoising technique, the temperature uncertainties of the raw data and the denoised data derived temperature profiles have been shown in Fig. 11 for comparison. The uncertainties are obtained by calculating the temperature standard deviation with a window of 5 m fiber length. The calculated uncertainty traces are then fitted by quadratic functions, and the estimated worst temperature uncertainties are 4.93 °C and 0.57 °C for the two cases without and with denoising, respectively. Thanks to the SNR enhancement enabled by the denoising technique, the uncertainty of temperature measurement has declined significantly. Therefore it indicates that the sensing range of ROTDR can be effectively extended by using the wavelet transform based

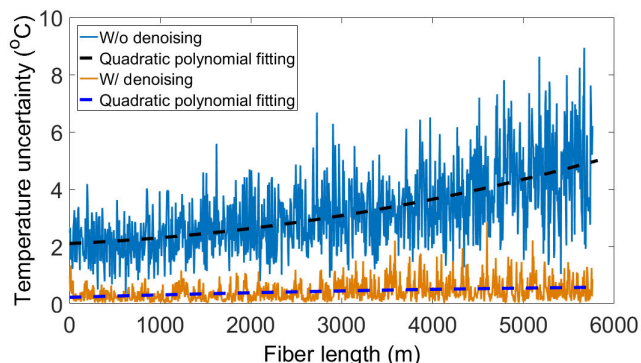


FIGURE 11. The temperature uncertainties of measurements as a function of fiber length that are obtained by processing the raw data and the denoised data, respectively.

denoising technique due to the enhanced SNR budget, which will further improve the sensing performance of the proposed hybrid system.

Finally, it is worth mentioning that the sensing range of the proposed hybrid system is essentially determined by ROTDR, because the spontaneous Raman scattering signal is much weaker than Rayleigh backscattering signal. Thanks to the SNR improvement that is enabled by wavelet transform based denoising, the sensing range of the hybrid system can be potentially extended remarkably, which will help to improve the overall performance of the sensing system. The measurement precision of both vibration and temperature in the hybrid system is limited by the SNR of the measured scattering traces, and the temperature precision of ROTDR is also related to the different wavelength-dependent losses (WDL) between the Raman Stokes and anti-Stokes signals. In addition, the sources of uncertainty of the hybrid system include the electric noise of the receiver, different WDL, the amplified spontaneous emission noise of the EDFA, etc.

IV. CONCLUSION

In conclusion, we propose and experimentally demonstrate a hybrid distributed fiber sensor that allows for simultaneous vibration and temperature monitoring by incorporating P-OTDR and ROTDR through SDM configuration in separate cores of a MCF. Instead of using a SMF, the embedded multiple spatial channels of MCF offer a novel way to enable simultaneous interrogations of both the spontaneous Raman and Rayleigh scattering signals in the sensing fiber, as a result the incompatible pump power levels issue in SMF can be effectively avoided. The temperature dependence of P-OTDR is also investigated in this work and it turns out that P-OTDR is much less sensitive to temperature than φ -OTDR, therefore it will allow for more accurate and reliable distributed vibration detection by using the proposed hybrid system, since the cross-sensitivity issue has been effectively mitigated. Furthermore, we also show the potential to extend sensing length of the hybrid system by using wavelet denoising technique. It shows that the proposed hybrid sensing system is pretty promising for

simultaneous distributed vibration and temperature monitoring of the pipelines, which can be applied in a variety of fields, especially in oil and gas industry.

ACKNOWLEDGMENT

The authors would like to acknowledge the support of Prof. Ming Tang of HUST and Dr. Weijun Tong of YOFC in providing the multicore fiber in the article.

REFERENCES

- [1] K. Miah and D. Potter, "A review of hybrid fiber-optic distributed simultaneous vibration and temperature sensing technology and its geophysical applications," *Sensors*, vol. 17, no. 11, p. 2511, Nov. 2017.
- [2] M. Niklès, "Long-distance fiber optic sensing solutions for pipeline leakage, intrusion, and ground movement detection," *Proc. SPIE*, vol. 7316, Apr. 2009, Art. no. 731602.
- [3] F. Tanimola and D. Hill, "Distributed fibre optic sensors for pipeline protection," *J. Natural Gas Sci. Eng.*, vol. 1, nos. 4–5, pp. 134–143, 2009.
- [4] A. Motil, A. Bergman, and M. Tur, "State of the art of Brillouin fiber-optic distributed sensing," *Opt. Laser Technol.*, vol. 78, pp. 81–103, Apr. 2016.
- [5] Z. Zhao, Y. Dang, M. Tang, L. Duan, M. Wang, S. Fu, W. Tong, and D. Liu, "Spatial-division multiplexed hybrid Raman and Brillouin distributed sensor employing multicore fiber," in *Proc. 25th Opt. Fiber Sensors Conf. (OFS)*, Jeju, South Korea, Apr. 2017, pp. 1–4.
- [6] X. Bao, D.-P. Zhou, C. Baker, and L. Chen, "Recent development in the distributed fiber optic acoustic and ultrasonic detection," *J. Lightw. Technol.*, vol. 35, no. 16, pp. 3256–3267, Aug. 15, 2017.
- [7] X. Fan, G. Yang, S. Wang, Q. Liu, and Z. He, "Distributed fiber-optic vibration sensing based on phase extraction from optical reflectometry," *J. Lightw. Technol.*, vol. 35, no. 16, pp. 3281–3288, Aug. 15, 2017.
- [8] Y. Muanenda, "Recent advances in distributed acoustic sensing based on phase-sensitive optical time domain reflectometry," *J. Sensors*, vol. 2018, May 2018, Art. no. 3897873.
- [9] Y. Koyamada, M. Imahama, K. Kubota, and K. Hogari, "Fiber-optic distributed strain and temperature sensing with very high measurand resolution over long range using coherent OTDR," *J. Lightw. Technol.*, vol. 27, no. 9, pp. 1142–1146, May 1, 2009.
- [10] J. Pastor-Graells, H. F. Martins, A. Garcia-Ruiz, S. Martin-Lopez, and M. Gonzalez-Herraez, "Single-shot distributed temperature and strain tracking using direct detection phase-sensitive OTDR with chirped pulses," *Opt. Express*, vol. 24, no. 12, pp. 13121–13133, Jun. 2016.
- [11] Y. Dang, Z. Zhao, M. Tang, C. Zhao, L. Gan, S. Fu, T. Liu, W. Tong, P. P. Shum, and D. Liu, "Towards large dynamic range and ultrahigh measurement resolution in distributed fiber sensing based on multicore fiber," *Opt. Express*, vol. 25, no. 17, pp. 20183–20193, 2017.
- [12] X. Lu, M. A. Soto, and L. Thévenaz, "Temperature-strain discrimination in distributed optical fiber sensing using phase-sensitive optical time-domain reflectometry," *Opt. Express*, vol. 25, no. 14, pp. 16059–16071, 2017.
- [13] Z. Z. Zhang and X. Bao, "Distributed optical fiber vibration sensor based on spectrum analysis of polarization-OTDR system," *Opt. Express*, vol. 16, no. 14, pp. 10240–10247, Jul. 2008.
- [14] N. Linze, P. Megret, and M. Wuilpart, "Development of an intrusion sensor based on a polarization-OTDR system," *IEEE Sensors J.*, vol. 12, no. 10, pp. 3005–3009, Oct. 2012.
- [15] C. Wang, Y. Zhou, H. Wu, C. Zhao, J. Tang, C. Zhou, S. Fu, P. Shum, and M. Tang, "Temporal depolarization suppressed POTDR system for quasi-distributed instantaneous intrusion sensing and vibration frequency measurement," *IEEE Photon. J.*, vol. 8, no. 2, Apr. 2016, Art. no. 6801514.
- [16] H. Wu, J. Liu, L. Lu, X. Sun, D. Atubga, and Y. Rao, "Multi-point disturbance detection and high-precision positioning of polarization-sensitive optical time-domain reflectometry," *J. Lightw. Technol.*, vol. 34, no. 23, pp. 5371–5377, Dec. 1, 2016.
- [17] C. Cao, F. Wang, Y. Pan, X. Zhang, X. Chen, Q. Chen, and J. Lu, "Suppression of signal fading with multi-wavelength laser in polarization OTDR," *IEEE Photon. Technol. Lett.*, vol. 29, no. 21, pp. 1824–1827, Nov. 1, 2017.
- [18] M. N. Alahbabi, Y. T. Cho, T. P. Newson, P. C. Wait, and A. H. Hartog, "Influence of modulation instability on distributed optical fiber sensors based on spontaneous Brillouin scattering," *J. Opt. Soc. Amer. B, Opt. Phys.*, vol. 21, no. 6, pp. 1156–1160, Jun. 2004.

- [19] H. F. Martins, S. Martin-Lopez, P. Corredera, P. Salgado, O. Frazão, and M. González-Herráez, "Modulation instability-induced fading in phase-sensitive optical time-domain reflectometry," *Opt. Lett.*, vol. 38, no. 6, pp. 872–874, 2013.
- [20] M. Alem, M. A. Soto, and L. Thévenaz, "Analytical model and experimental verification of the critical power for modulation instability in optical fibers," *Opt. Express*, vol. 23, no. 23, pp. 29514–29532, 2015.
- [21] M. N. Alahbabi, Y. T. Cho, and T. P. Newson, "Simultaneous temperature and strain measurement with combined spontaneous Raman and Brillouin scattering," *Opt. Lett.*, vol. 30, no. 11, pp. 1276–1278, 2005.
- [22] Z. Zhao, "Spatial-division multiplexed hybrid Raman and Brillouin optical time-domain reflectometry based on multi-core fiber," *Opt. Express*, vol. 24, no. 22, pp. 25111–25118, 2016.
- [23] Z. Zhao, Y. Dang, M. Tang, L. Wang, L. Gan, S. Fu, C. Yang, W. Tong, and C. Lu, "Enabling simultaneous DAS and DTS through space-division multiplexing based on multicore fiber," *J. Lightw. Technol.*, vol. 36, no. 24, pp. 5707–5713, Dec. 15, 2018.
- [24] C. Wang, R. Liao, W. Chen, M. Tang, S. Fu, J. Tang, C. Zhou, and D. Liu, "Simplex coded polarization optical time domain reflectometry system," *Opt. Express*, vol. 25, no. 5, pp. 5550–5558, 2017.
- [25] H. Dong, M. Tang, and Y. Gong, "Measurement errors induced by deformation of optical axes of achromatic waveplate retarders in RRFP Stokes polarimeters," *Opt. Express*, vol. 20, no. 24, pp. 26649–26666, Nov. 2012.
- [26] Z. Zhao, Z. Liu, M. Tang, S. Fu, L. Wang, N. Guo, C. Jin, H.-Y. Tam, and C. Lu, "Robust in-fiber spatial interferometer using multicore fiber for vibration detection," *Opt. Express*, vol. 26, no. 23, pp. 29629–29637, 2018.
- [27] X. Wang, J. Hu, F. Wang, Y. Yong, Y. Zhang, M. Xue, X. Zhang, and S. Pan, "Multi-vibration detection by probe pulses with ergodic SOPs in a POTDR system," *Opt. Express*, vol. 26, no. 22, pp. 28349–28362, 2018.
- [28] M. A. Soto, J. A. Ramirez, and L. Thévenaz, "Intensifying the response of distributed optical fibre sensors using 2D and 3D image restoration," *Nature Commun.*, vol. 7, Mar. 2016, Art. no. 10870.
- [29] Q. Pan, L. Zhang, G. Dai, and H. Zhang, "Two denoising methods by wavelet transform," *IEEE Trans. Signal Process.*, vol. 47, no. 12, pp. 3401–3406, Dec. 1999.
- [30] S. D. Ruikar and D. D. Doye, "Wavelet based image denoising technique," *Int. J. Adv. Comput. Sci. Appl.*, vol. 2, no. 3, pp. 49–53, Mar. 2011.
- [31] H. Wu, L. Wang, Z. Zhao, N. Guo, C. Shu, and C. Lu, "Brillouin optical time domain analyzer sensors assisted by advanced image denoising techniques," *Opt. Express*, vol. 26, no. 5, pp. 5126–5139, Mar. 2018.



XUEFENG WANG received the B.S. degree from the School of Computer and Electronic Information, Guangxi University, Nanning, China, in 2015, and the M.Eng. degree from the School of Optical and Electronic Information, Huazhong University of Science and Technology (HUST), Wuhan, China, in 2017, where he is currently pursuing the Ph.D. degree. His current research interest includes optical fiber sensing.



RUOLIN LIAO received the B.S. and M.Eng. degrees from the School of Optical and Electronic Information, Huazhong University of Science and Technology (HUST), Wuhan, China, in 2014 and 2016, respectively, where he is currently pursuing the Ph.D. degree.

His current research interests include microwave photonics and fiber sensing.



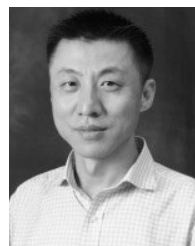
YUNLI DANG received the B.Eng. degree in measurement and control technology and instrumentation from Northeastern University, Shenyang, China, in 2015, and the M.Sc. degree in optical engineering from the School of Optical and Electronic Information, Huazhong University of Science and Technology, Wuhan, China, in 2018.

She joined Yangtze Optical Fiber and Cable Joint Stock Limited Company (YOFC), in 2018. Her research interests include optical fiber sensing and special optical fibers.



ZHIYONG ZHAO received the B.Eng. and Ph.D. degrees from the Huazhong University of Science and Technology (HUST), Wuhan, China, in 2012 and 2017, respectively.

He was a joint Ph.D. Student with the École polytechnique fédérale de Lausanne (EPFL), Lausanne, Switzerland, from October 2014 to October 2015. He also stayed half a year as a Research Assistant with the School of Electrical and Electronic Engineering, Nanyang Technological University (NTU), Singapore. Since June 2017, he has been a Postdoctoral Fellow with the Department of Electronic and Information Engineering, The Hong Kong Polytechnic University, Kowloon, Hong Kong. His current research interests include optical fiber sensing, optical fiber devices, special optical fibers, and nonlinear fiber optics.



CHAO LU received the B.Eng. degree in electronic engineering from Tsinghua University, China, in 1985, and the M.Sc. and Ph.D. degrees from the University of Manchester, in 1987 and 1990, respectively. He joined the School of Electrical and Electronic Engineering, Nanyang Technological University (NTU), Singapore, in 1991, where he has been a Lecturer, a Senior Lecturer, and an Associate Professor, until 2006. From June 2002 to December 2005, he was seconded to the Institute

for Infocomm Research, Agency for Science, Technology and Research (A*STAR), Singapore, as a Program Director and a Department Manager, leading a research group in the area of optical communication and fiber devices. He joined the Department of Electronic and Information Engineering, The Hong Kong Polytechnic University, as a Professor, in 2006, where he is the Chair Professor of fiber optics. He has published more than 300 articles in major international journals, such as *Optics Express*, *Optics Letters*, the *IEEE PHOTONIC TECHNOLOGY LETTERS*, and the *IEEE/OSA JOURNAL OF LIGHTWAVE TECHNOLOGY*. He has been organizer or technical program committee member of many international conferences. His current research interests include high capacity transmission techniques for long haul and short reach systems and distributed optical sensing systems. In addition to academic research work, he has had many industrial collaborative research projects and has a number of awarded patents. He is a Fellow of the Optical Society (OSA).

• • •